Published in final edited form as:
Cancer Res. 2007 May 15; 67(10): 4605–4619. doi:10.1158/0008-5472.CAN-06-3619.

Fundamental Differences in Cell Cycle Deregulation in Human Papillomavirus–Positive and Human Papillomavirus–Negative Head/Neck and Cervical Cancers

Dohun Pyeon[1,2], **Michael A. Newton**[3], **Paul F. Lambert**[1], **Johan A. den Boon**[1,2], **Srikumar Sengupta**[1,2], **Carmen J. Marsit**[6], **Craig D. Woodworth**[7], **Joseph P. Connor**[4], **Thomas H. Haugen**[8], **Elaine M. Smith**[9], **Karl T. Kelsey**[6], **Lubomir P. Turek**[8], and **Paul Ahlquist**[1,2,5]

[1]McArdle Laboratory for Cancer Research, University of Wisconsin-Madison, Madison, Wisconsin

[2]Institute for Molecular Virology, University of Wisconsin-Madison, Madison, Wisconsin

[3]Department of Statistics and of Biostatistics and Medical Informatics, University of Wisconsin-Madison, Madison, Wisconsin

[4]Department of Obstetrics and Gynecology, University of Wisconsin-Madison, Madison, Wisconsin

[5]Howard Hughes Medical Institute, University of Wisconsin-Madison, Madison, Wisconsin

[6]Departments of Genetics and Complex Diseases, Harvard School of Public Health, Boston, Massachusetts

[7]Department of Biology, Clarkson University, Potsdam, New York

[8]Department of Pathology, Veterans Affairs Medical Center, University of Iowa, Iowa City, Iowa

[9]Department of Epidemiology, University of Iowa, Iowa City, Iowa

Abstract

Human papillomaviruses (HPV) are associated with nearly all cervical cancers, 20% to 30% of head and neck cancers (HNC), and other cancers. Because HNCs also arise in HPV-negative patients, this type of cancer provides unique opportunities to define similarities and differences of HPV-positive versus HPV-negative cancers arising in the same tissue. Here, we describe genome-wide expression profiling of 84 HNCs, cervical cancers, and site-matched normal epithelial samples in which we used laser capture microdissection to enrich samples for tumor-derived versus normal epithelial cells. This analysis revealed that HPV^+ HNCs and cervical cancers differed in their patterns of gene expression yet shared many changes compared with HPV^- HNCs. Some of these shared changes were predicted, but many others were not. Notably, HPV^+ HNCs and cervical cancers were found to be up-regulated in their expression of a distinct and larger subset of cell cycle genes than that observed in HPV^- HNC. Moreover, HPV^+ cancers overexpressed testis-specific genes that are normally expressed only in meiotic cells. Many, although not all, of the hallmark differences between HPV^+ HNC and HPV^- HNC were a direct consequence of HPV and in particular the viral E6 and E7 oncogenes. This included a novel association of HPV oncogenes with testis-specific gene expression. These findings in primary

Requests for reprints: Paul Ahlquist, McArdle Laboratory for Cancer Research, University of Wisconsin-Madison, 1525 Linden Drive, Madison, WI 53706. Phone: 608-263-5916; Fax: 608-265-9214; ahlquist@wisc.edu.

Note: Supplementary data for this article are available at Cancer Research Online (http://cancerres.aacrjournals.org/).

P. Ahlquist is an investigator of the Howard Hughes Medical Institute.

human tumors provide novel biomarkers for early detection of HPV^+ and HPV^- cancers, and emphasize the potential value of targeting E6 and E7 function, alone or combined with radiation and/or traditional chemotherapy, in the treatment of HPV^+ cancers.

Introduction

Human papillomaviruses (HPV) are DNA viruses that infect and replicate in cutaneous and mucosal epithelia, causing benign lesions (1). High-risk, mucosotropic HPV genotypes, including HPV16, HPV18, and HPV31, are causally associated with a variety of anogenital squamous cell carcinomas, including cancers of the lower female reproductive tract, penis, and anus (1). In particular, high-risk HPVs are associated with nearly all cervical cancers, a leading cause of cancer death in women worldwide despite the effectiveness in developed countries of screening for early detection of precancerous lesions (1). Prophylactic HPV vaccines should eventually reduce infections by the most prevalent high-risk HPVs, but do not cover all high-risk HPVs. These vaccines also lack therapeutic effects and so will not affect existing HPV infections that will produce cervical cancer for decades hence.

More recently, high-risk HPVs have also been associated with head and neck cancer (HNC; refs. 2,3). HNC, which arises in mucosal epithelia lining the mouth, oropharynx, and throat, is the sixth most common cancer in United States, with a survival rate of ~50% (4). Although nearly all cervical cancers are caused by HPV only 20% to 30% of HNCs are associated with HPV (2,3); the rest are linked to other risk factors, including tobacco and alcohol. This varied etiology of HNCs provides unique opportunities to study viral contributions to cancer by comparing HPV-associated and HPV-independent cancers in the same anatomic sites. Additionally, HPV^+ cervical cancers allow identifying similarities or differences among HPV-associated cancers at distinct anatomic sites.

Recent gene expression profiling studies of HNCs identified four potential subgroups of the HNC population studied (5) and signatures potentially associated with increased risk for metastasis (6) or recurrent disease (7). Although these results contributed greatly to the understanding of HNC, many issues remain because these studies used nonlaser microdissected samples, including tumor and nontumor tissue, analyzed only a fraction of human genes (~12,000–14,000 genes), and did not determine tumor HPV status. Slebos et al. (8) identified some gene expression differences between HPV^+ and HPV^- HNCs, although the conclusions of this study were limited by a lack of comparison with normal head and neck tissue or HPV^+ cervical cancer.

The oncogenic potential of HPV is believed to reside largely in viral oncogenes E6 and E7, which block tumor-suppressor functions of p53 and Rb, respectively (9). For example, E7-Rb interaction releases E2F family transcription factors to induce transcription of cell cycle-regulated genes, such as *cyclin E* (10) and *MCM*s (11). Beyond p53 and Rb, however, E6 and E7 are multifunctional proteins for which numerous interaction partners and functions have been proposed (12,13). Moreover, in mouse models, the relative oncogenic contribution of E6 and E7 varies dramatically between tissues (14). Additionally, although the oncogenic mechanisms of natural human cancers are complex, most studies have been done in simple tissue culture or animal models based on unnatural overexpression of one or more HPV oncogenes. Thus, despite significant insights into HPV oncogene function, many important questions remain about E6 and E7 effects in HPV^+ HNC, their modulation by other HPV genes and additional genetic changes, and the possible relation of these effects to those in cervical cancer and HPV^- HNC.

To address these important questions, we investigated gene expression patterns in HPV^+ and HPV^- HNCs, cervical cancers, and normal epithelia from both sites. Cancer cells were laser

microdissected from the surrounding tissue to define tumor-specific gene expression and RNAs were hybridized to genome-wide human microarrays (>54,000 probe sets) and custom HPV microarrays, defining HPV status and genotype. We found that although the overall gene expression profiles of cervical cancer, HPV^+ HNC, and HPV^- HNC are readily distinguishable, expression patterns of specific gene subgroups, including a range of cell cycle–associated genes and certain testis-specific genes, are shared between HPV^+ cancers of the head and neck region and the cervix. Our findings also revealed that HPV^+ cancers show significantly increased expression of proliferation markers than HPV^- cancers, providing a mechanistic explanation for recent clinical results (15) that HPV^+ HNCs are more responsive to radiotherapy than HPV^- HNCs. These and other results herein provide new insights in understanding, diagnosing, and potentially treating HPV-associated versus HPV-negative cancers.

Materials and Methods

Tissue samples

Fifteen and 27 HNC samples were from the University of Iowa and Harvard School of Public Health, respectively. Five and nine HNN samples were from the University of Iowa and the National Disease Research Interchange, respectively (Supplementary Table S1). Cervical cancer and normal cervical samples were from the Gynecologic Oncology Group. Patient information is presented in Table 1 and Supplementary Table S1. All tissue samples were fresh frozen in liquid nitrogen and collected with patient consent under approval of the institutional review boards from all participating institutions. Also, all the tumor samples are primary resections collected before the initiation of chemotherapy or radiotherapy. Each sample was processed and RNA was prepared and labeled as described in Supplementary Methods.

Human and HPV microarrays

Human gene expression was profiled using Affymetrix U133 Plus 2.0 arrays (Affymetrix). For HPV detection and genotyping, 70-mer oligonucleotide probes with a T_M of 80°C (Supplementary Methods) were designed using Oligowiz 1.0 (16), purchased from MWG-Biotech, and spotted in quadruplicate on epoxy glass slides (TeleChem International, Inc.) with BioRobotics MicroGrid II (Genomic Solutions). HPV array hybridization was carefully optimized using RNA from known HPV^+ and HPV^- keratinocyte cell lines (Supplementary Methods). HPV arrays were hybridized with biotin-labeled cRNA, processed as in Supplementary Methods, and scanned using an Agilent DNA microarray scanner (Agilent). Images were analyzed using Axon GenePix Pro 5.1 software (Molecular Devices). Ten micrograms of cRNA were used for Affymetrix microarray hybridization and scanning at the University of Wisconsin Biotechnology Gene Expression Center. To obtain statistically significant sample number in each group while minimizing unnecessary sample processing and microarray use, we selected HNC samples based in part on HPV status.

Statistical analysis

Tools in R (17) and Bioconductor (18) were adapted for statistical analysis. Probe set summary measures were computed by robust multiarray averaging (19) applied to the combined set of 84 microarrays. Average base 2 log expression was used to summarize the expression of each probe set within a tissue class. Multidimensional scaling allowed global (i.e., averaged over the genome) comparisons between classes, and class-restricted nonparametric bootstrap sampling (20) was used to measure the significance of observed differences between global correlations computed on pairs of tumor classes. Permutation testing was used to confirm that each measured correlation was significantly nonzero. The primary analysis of differential gene expression at the probe set level was done in three

pairwise comparisons: Tumor versus normal, HPV^+ versus HPV^-, and HNC versus cervical cancer. Fold changes and *t* statistics were used to identify differentially expressed probe sets; the latter were converted to *q* values to control false-discovery rate (21).

Enrichment of gene ontology (GO) categories for differentially expressed genes was measured using random-set testing methods (22,23). Briefly, the proportion of significantly altered genes and the average log fold change for all genes in each of 2,760 GO categories were compared, respectively, to their distributions on a random set of genes to obtain standardized enrichment *Z* scores. A category was considered significantly enriched for altered genes if both of these *Z* scores exceeded 4 (nominal $P = 3 \times 10^{-5}$). Calculations used version 1.0 of the R package *allez*, and the October 2005 build of Bioconductor package *hgu133plus2*. The same *Z* score standardization applied to class-averaged expression profiles (above) was used to compute GO profiles for each tissue class. These were correlated between classes to assess the similarity of tissue classes.

We developed a parametric testing strategy (20) to evaluate the significance of apparent profile-defined tumor subgroups of the HPV^+ HNC tumors (Supplementary Fig. S4A–C). Specifically, a multivariate normal distribution was fit to data from the 16 HPV^+ HNC arrays using $n = 100$ genes most differentially expressed between HPV^+ cancers and HPV^- cancers (Fig. 2A). The rationale was that such a unimodal Gaussian distribution represents a baseline null hypothesis of no actual subgrouping from which the significance of apparent subgroups could be gauged. Because the sample covariance matrix was rank deficient, we used an empirical Bayes estimate of covariance (24) and repeatedly (10^4 times) sampled multivariate random *n*-vectors from a centered normal population with this covariance matrix. Using each bootstrap sample, we divided the 16 tumors according to the subgrouping derived at the penultimate merge of a hierarchical cluster analysis. Each split was scored by the average of the squared *t* statistics between the two subgroups, which is large if the subgroups are relatively well separated. The average squared *t* statistic on the subgroups identified by hierarchical clustering of the actual data was compared with the distribution of such scores derived, as above, on the null hypothesis that the profiles emerge from a single, multivariate normal, population, and a *P* value was computed. To assess sensitivity, we repeated the calculations at a range of gene set sizes *n*.

Tissue culture, quantitative reverse transcriptase-PCR, Western blotting, and immunohistochemistry were done as described in Supplementary Methods.

Results

Tissue samples, microarray profiling, and HPV status

Eighty-four samples including 42 HNCs, 14 head and neck normals (HNN), 20 cervical cancers, and 8 cervical normals were cryosectioned, and selected sections were stained with H&E, verified free of autolysis and freezing artifacts, and analyzed histopathologically. Relevant patient information is summarized in Table 1 and Supplementary Table S1. All tumor samples were collected before chemotherapy or radiotherapy. For all normal tissues and tumors with <90% cancer cells (61 of 84), laser microdissection was done to capture normal epithelial or tumor cells, respectively (Supplementary Fig. S1). Complementary RNA (cRNA) was prepared and hybridized to Affymetrix U133 Plus 2.0 microarrays containing oligonucleotide probes for all known expressed human mRNAs. Normalization was done as described in Materials and Methods. Resulting microarray data were deposited to the National Center for Biotechnology Information Gene Expression Omnibus database under general accession number GSE6791 and sample accession numbers in Supplementary Table S1.

HPV status and genotype were determined by hybridization to custom-made 70-mer oligonucleotide microarrays containing probes for all 37 known mucosotropic HPV genotypes plus positive and negative control probes. These microarrays were sufficiently sensitive to detect HPV in cell lines harboring a few extrachromosomal copies or a single integrated copy of HPV DNA. No normal tissue showed any significant HPV signal; however, consistent with prior findings (3), 16 of 42 HNCs harbored HPV (13 HPV16, two HPV33, and one HPV18; Table 2). About half of cervical cancers were HPV16 positive, with lesser numbers carrying HPV genotypes 18, 31, 33, 35, 58, or 66 (Table 2). Three of 20 cervical cancers hybridized well to control cell mRNA probes but showed no detectable HPV signal. PCR with consensus HPV L1 primers MY09-MY11 (25) confirmed absence of detectable HPV DNA in these samples (Supplementary Fig. S2).

Because these samples shared some expression patterns with HPV^+ cervical cancer and HNCs (see below), they may contain HPV, possibly with sequence variations inhibiting detection by these sequence-specific methods (26). However, varying the HPV status assigned to these three cervical cancers had only minimal effects on the gene expression signature differentiating HPV^+ and HPV^- cancers. Comparisons of HPV^+ and HPV^- cancers with these samples included as HPV^- cervical cancer, as HPV^+ cervical cancer, or excluded all revealed HPV-specific expression signatures dominated by a robust common core of nearly 140 genes. The analysis below reports HPV^+ and HPV^- cancer comparisons based on the original HPV^- assignment of these cervical cancers, because this yielded the best-conserved core expression signature (137 genes), whereas the alternate assumptions each added some additional genes whose differential expression levels were not as well conserved across the analyses.

Gene expression relationships among HPV^+ and HPV^- HNCs and cervical cancers

Global pairwise comparisons of complete mRNA expression profiles between all tumor and normal sample classes were done by multidimensional scaling (27). This analysis (Fig. 1A) measures for each pair of tumor and normal classes the distances between class-averaged log 2 expression levels over all 54,675 Affymetrix probe sets. Not surprisingly, the most closely related classes were HPV^+ HNC and HPV^- HNC (average distance, 0.17). Notably, the next closest classes were the two HPV^+ cancers, HPV^+ HNC and HPV^+ cervical cancer, whose distance of 0.21 was closer than either to its corresponding normal (0.29, 0.53).

The global effect of virus-specific and tissue-specific factors is further illustrated in Fig. 1B, which compares for paired tumor classes the log 2 average expression levels, relative to corresponding normals, of all probe sets. The indicated Pearson correlation coefficients confirm that the highest correlation is between HPV^+ HNC and HPV^- HNC ($R = 0.81$). The substantial correlation between HPV^+ HNCs and HPV^+ cervical cancers ($R = 0.58$), well above HPV^+ cervical cancers and HPV^- HNCs ($R = 0.46$), again implies a substantial role for virus-dependent, tissue-independent factors in gene expression changes. HPV^+ HNC versus HPV^+ cervical cancer correlation exceeds the HPV^- HNC versus HPV^+ cervical cancer correlation in more than 90% of bootstrap sampled data sets, and all correlations were significant by permutation analysis. Thus, both HPV status and tissue type contribute to the relatedness and distinction of HPV^+ HNCs, HPV^- HNCs, and HPV^+ cervical cancers.

To offset variation in probe set–level measurements, we did similar correlation analyses on fold changes averaged over GO gene classes rather than individual probe sets, reinforcing the findings above (Supplementary Fig. S3A).

Although HPV^+ HNC and HPV^- HNC exhibited generally high positive correlation in gene expression changes from normal, many genes had altered expression between these two classes. Figure 1B highlights 47 genes selectively up-regulated (red points) and 45 genes

selectively down-regulated (blue points) by >2.6-fold in HPV^+ HNC relative to HPV^- HNC (see also Supplementary Table S3A and S3B). Notably, for genes that were highly up-regulated in HPV^+ HNC relative to HPV^- HNC, parallel comparison of expression levels between HPV^+ HNC and cervical cancer shifted their distribution in the plot dramatically rightward, revealing substantial correlated expression in these two HPV^+ cancers (*red arrow* and *points* in Fig. 1B, *middle*). Conversely, genes that were significantly down-regulated in HPV^+ HNC relative to HPV^- HNC showed a substantial but opposite leftward shift into greater correlation in a comparison plot of expression levels between HPV^+ HNC and cervical cancer (*blue arrow* and *points* in Fig. 1B, *middle*). Thus, the tumor-specific expression changes in these genes correlated much more strongly with the presence of HPV than the tissue site.

To further analyze gene expression changes based on tumor/normal, HPV^+/HPV^-, and HNC/cervical cancer differences, we identified for each comparison differentially expressed genes with fold change >2 and *t* test $q < 0.001$. By these criteria, as shown in Fig. 1C, 1,701 and 243 genes were up- and down-regulated, respectively, in tumors relative to normals; on the other hand, 124 and 13 genes were up- and down-regulated in HPV^+ relative to HPV^- cancers, and 256 and 35 genes were up- and down-regulated in cervical cancer relative to HNC.

More specifically, in tumor/normal comparisons (Supplementary Fig. S3B; Supplementary Table S5), HPV^+ HNC, HPV^- HNC, and cervical cancer all were up-regulated relative to normals for a gene set I, including keratins (*KRT8, KRT17, KRT18*), caveolin (*CAV2*), IFNα-inducible protein 6-16 (*G1P3*), matrix metallopeptidase 12 (*MMP12*), collagens (*COL4A1, COL4A2*), and phospholipid scramblase 1 (*PLSCR1*), and down-regulated for another set II, including other keratins (*KRT4, KRT13, KRT15*), programmed cell death 4 (*PDCD4*), protein tyrosine kinase 6 (*PTK6*), epithelial membrane protein 1 (*EMP1*), extracellular matrix protein 1 (*ECM1*), interleukin 1 receptor (*IL1R2*), and transglutaminase 3 (*TGM3*).

Relative to HPV^- HNC (Fig. 2A; Table 3), HPV^+ HNC and cervical cancer showed significantly increased expression of gene set III, including PC4/SFRS1-interacting protein 1 (*PSIP1*), V-myb (*MYB*), synaptogyrin 3 (*SYNGR3*), SWI/SNF-related, matrix-associated, actin-dependent regulator of chromatin (*SMARCA2*), synaptonemal complex protein 2 (*SYCP2*), p16 (*CDKN2A*), lymphoid-specific heli-case (*HELLS*), and testicular cell adhesion molecule 1 (*TCAM1*), whereas expression was decreased for gene set IV, including parathyroid hormone-like hormone (*PTHLH*), cortactin (*CTTN*), kallikreins (*KLK8, KLK10*), cyclin D1 (*CCND1*), caveolin 1 (*CAV1*), and defensin β4 (*DEFB4*). At the GO category level (Supplementary Table S4A), HPV^+ cancers were up-regulated relative to HPV^- cancers for annotations related to DNA replication and cell cycle, and down-regulated in genes involved in epidermal development and hormone activity.

In comparison between cervical cancer and HNC (Fig. 2B; Supplementary Table S6), cervical cancers showed significantly up-regulated expression of gene sets V and VII, including estrogen receptor 1 (*ESR1*), keratin 19 (*KRT19*), X (inactive)–specific transcript (*XIST*), and zinc finger protein 367 (*ZNF367*), whereas HNC showed increased expression of gene set VI (Fig. 2B; Supplementary Table S6), including dermatopontin (*DPT*), desmocollin 1 (*DSC1*), melanoma antigen A12 (*MAGEA12*), and chromosome Y open reading frame 15B (*CYorf15B*).

A distinct subgroup in HPV^+ cancers

Hierarchical clustering of differentially expressed genes between HPV^+ and HPV^- cancers revealed two subgroups of HPV^+ cancers (Supplementary Fig. S4A and S4B). These subgroups (α and β) were not correlated with any identified sample characteristics including

anatomic site, age, or clinical stage (Supplementary Table S1A) and were robustly preserved when the grouping was repeated using different agglomeration methods for clustering and varying numbers of differentially expressed genes.

The smaller subgroup, a, showed high up-regulation of a set of B lymphocyte/lymphoma–related genes, including baculoviral IAP repeat 3 (*BIRC3*), butyrophilin-like 9 (*BTNL9*), DKFZ P564O0823, homeobox C6 (*HOXC6*), and B-cell chronic lymphocytic leukemia/lymphoma 11A (*BCL11A*; Supplementary Fig. S4C; Supplementary Table S7). B cell–related gene expression by this tumor subgroup was not due to tumor-infiltrating B cells, because there was no correlation between this subgroup and expression of CD19, CD20, and immunoglobulins, which are expressed in B cells throughout most or all circulating stages (28).

Subgroup α also was up-regulated relative to other HPV^+ cancers for genes expressed by endothelial cells, including vascular cell adhesion molecule 1 (*VCAM1*) and zinc finger protein 62 (*ZNF62*) and down-regulated for genes, including several small proline-rich proteins (*SPRR1A* and *SPRR2A*), keratins (*KRT6B* and *KRT16*), and gap junction proteins (*GJB2* and *GJB6*; Supplementary Fig. S4C; Supplementary Table S7). Expression of synaptopodin (*SYNPO2*), an important regulator of cell migration (29), was increased >20-fold in this subgroup relative to other HPV^+ cancers, suggesting potentially increased invasiveness.

Due to variations among microarray platforms and methods, reproducibility of expression profiling has been one of the biggest challenges in microarray studies of cancer (30). Chung et al. (5) recently reported dividing 60 HNCs into four subgroups by gene expression patterns. However, clustering our samples based on the genes reported as differentially expressed signatures of these four subgroups revealed little significant correlation. Possible causes for this lack of correlation include use of whole samples in the prior study versus selectively microdissected samples here, differences in the microarray platforms used, or limitations in sample group sizes in these studies. Supplementary Fig. S5A shows the best association of our HNC samples into four groups based on the prior signature gene sets. Although weak, the B lymphocyte/lymphoma–related subset α identified in Supplementary Fig. S4 showed the most similarity for Chung et al.'s subgroup 2, in that most genes in Chung et al.'s set E were down-regulated and, for two of the six relevant tumors (*HNC005, HNC012*), some genes in set F were up-regulated, primarily including mesenchymal markers associated with poorer clinical outcomes (5,31): syndecan, vimentin, and some collagens (Supplementary Table S8).

HPV^+ and HPV^- cancers are activated in different components of the cell cycle pathway

E7 oncoproteins of high-risk HPVs induce DNA replication and mitosis by multiple mechanisms, including interacting with pRb, HDACs, and other factors to activate cell cycle–regulated transcription factors such as E2F (32–34). However, the extent of the resulting gene expression changes, the full contributions of other HPV genes and additional genetic changes to oncogenesis, and the relation of these effects to those in HPV^- HNC have not been determined. To test for differential expression in HPV^+ versus HPV^- cancers, we examined cell cycle–related genes based on GO classification. A significant subset of cell cycle–regulated genes was differentially expressed in HPV^+ HNC and cervical cancer relative to HPV^- HNC (Fig. 3A; Table 4). As shown in Fig. 3B, HPV^- HNCs up-regulated, relative to HPV^+ cancers, a small set of cell cycle–specific genes, including cyclin D1/D2 (*CCND1* and *CCND2*; G_1 associated) and cyclin A1 *(CCNA1*; Fig. 3A, set VIII, and 3B). By contrast, HPV^+ cancers up-regulated, relative to HPV^- HNC, a much larger set of cell cycle–specific genes such as cyclin E2 (*CCNE2*; G_1 associated), cyclin B1 (*CCNB1*; G_2 associated), and multiple MCMs (Fig. 3A, set IX, and B). Among these, many genes that

enhance DNA replication and cell mitosis, including proliferating cell nuclear antigen (*PCNA*), *E2Fs*, *cdc2*, *cdc7*, and *MCMs* were significantly up-regulated in HPV^+ HNC and cervical cancer relative to HPV^- HNC, implying that the HPV^+ cancers were more active in cell division.

A subset of these genes were analyzed by quantitative reverse transcriptase-PCR (qRT-PCR) with total RNA extracted from naturally immortalized human keratinocyte lines NIKS-16 and NIKS, which have and lack an extrachromosomal HPV16 genome, respectively (35). In keeping with the microarray results, *p16*, *cdc7*, origin recognition complex 1 (*ORC1*), kinetochore-associated protein (*KNTC1*), *MCM6*, cyclin B1 (*CCNB1*), *BUB1*, *cdc2*, and *cdc20* were highly up-regulated by HPV16, whereas cyclin A1 (*CCNA1*) was down-regulated (Fig. 3C). Because the NIKS-16 cells were only five to six passages after stable HPV16 transfection, these results indicate that HPV deregulates a subset of cell cycle–related genes soon after being acquired by cells. To eliminate possible effects of the prior spontaneous immortalization of NIKS cells, we measured gene expression levels in normal (i.e., early passage) cervical epithelial cells transduced with HPV16 E6 and/or E7 oncogenes. The results confirmed NIKS data, showing an up-regulation of *CCNB1*, *cdc2*, *ORC1*, and *p16* by HPV16 E6 and E7 expression (Supplementary Fig. S6). Moreover, immunohistochemistry showed that tumor cells in HPV^+ cancers expressed significantly ($P < 0.001$) higher levels of PCNA protein than HPV^- tumor cells (Fig. 4). In addition, PCNA protein levels were highly correlated with cell cycle–related gene expression levels (Supplementary Table S9). Together, these results indicate that HPV acts in HPV^+ HNCs and cervical cancers to deregulate the cell cycle pathway in shared ways that are markedly distinct from HPV^- HNCs.

Up-regulation of novel testis antigens in HPV^+ cancers

Genes highly up-regulated in HPV^+ cancers relative to HPV^- HNC included two testis-specific genes not normally expressed in somatic cells, *SYCP2* and *TCAM1* (Fig. 2A; Table 3). qRT-PCR showed that SYCP2 and TCAM1 expression were increased >15- and >100,000-fold, respectively, in $HPV16^+$ NIKS-16 relative to $HPV16^-$ NIKS cells (Fig. 5A). SYCP2 also was detected at the protein level in NIKS-16 but not NIKS cells (Fig. 5B). Comparative studies with NIKS16ΔE7 cells (Fig. 5A) and in primary cervical keratinocytes with or without HPV16 E6 and/or E7 expression (Fig. 5C) showed that SYCP2 and TCAM1 expression are synergistically up-regulated by E6 and E7.

A third testis-specific gene up-regulated in HPV^+ HNC and cervical cancer relative to HPV^- HNC was stromal antigen 3 (*STAG3*; Table 3). Unlike *SYCP2* and *TCAM1*, *STAG3* mRNA was not up-regulated in early passage NIKS-16 relative to NIKS cells nor in early passage HPV^+ W12 cells (Fig. 5D). However, in three HPV^+ cervical carcinoma cell lines (CaSki, HeLa, and SiHa), STAG3 expression was increased 6- to 40-fold over NIKS. Additionally, we observed passage-dependent increased expression of STAG3 in cervical epithelial cells harboring HPV16 (cervical keratinocytes +HPV16; Fig. 5D). These data suggest that *STAG3* induction was not an immediate effect of the virus, but is rather a delayed, passaging-dependent response.

Discussion

Here, we defined molecular differences and similarities among HPV^+ HNCs, HPV^- HNCs, and cervical cancers. In particular, HPV^+ HNC and cervical cancer differentially expressed significant gene sets relative to HPV^- HNC, including cell cycle regulatory genes and testis-specific genes with mechanistic, diagnostic, and therapeutic implications. Although current clinical practice does not differentiate HNC treatment based on etiologic differences, our results show that cell cycle deregulation and other underlying characteristics of HPV^+ HNCs

are greatly dissimilar to HPV$^-$ HNCs, but similar to cervical cancers, implying that therapeutic approaches can and should be optimized independently for HPV$^+$ and HPV$^-$ cancers.

Up-regulation of cell cycle–related genes in HPV$^+$ HNC and cervical cancer

An important finding of this study is that HPV$^+$ and HPV$^-$ cancers differentially express a large subset of cell cycle regulatory genes (Fig. 3A and B). For example, HPV$^+$ cervical cancers and HNCs overexpressed cyclins E and B, whereas HPV$^-$ HNCs overexpressed cyclins D and A. A recent study of only HPV$^+$ HNC and HPV$^-$ HNC reported only a few of the cell cycle regulators identified here as differentially expressed (8). However, our analysis of microarray data from that study shows that the same subset of cell cycle genes shown in Fig. 3A above were differentially expressed in HPV$^+$ versus HPV$^-$ cancers, confirming these results in an independent patient population (Supplementary Fig. S5B). Our experiments in keratinocytes, including cervical epithelial cells, lacking or transfected/transduced with HPV16, confirmed that HPV induced the observed characteristic expression pattern of cell cycle genes (Fig. 3C; Supplementary Fig. S6).

Strikingly, many of the cell cycle regulatory genes overexpressed in HPV$^+$ cancers are known or suspected to be responsive to E2F family transcription factors activated by HPV E7. These include MCMs (32), ORC (36), cdc7 (37), PCNA (38), cdc2 (39), and cyclin A (40). The distinct pattern of cell cycle regulatory gene expression in HPV$^+$ cancers thus likely reflects E7-E2F interactions (34). A role for E7 in up-regulating two of these cell cycle genes (*MCM7* and *cyclin E*) has been shown in a mouse model for HPV-associated cervical cancer (34), and these two E2F-responsive genes are also up-regulated in a new mouse model for HPV-associated HNC (41). Interestingly, in the mouse models for HPV-associated cervical cancer and HNC, E7 dominates over other HPV oncogenes in tumor induction (14).[10] Thus, multiple, independent observations imply that the cell cycle deregulation in HPV$^+$ human cancers at least partly reflects E7 action.

Perhaps the most striking difference in cell cycle regulatory gene expression was seen with *cyclin D1/CCND1* and *p16/Ink4a/CDKN2A*. In HPV$^+$ cancers, p16 was expressed at high levels and cyclin D1 at low levels, with the converse in HPV$^-$ cancers (Fig. 3A). A recent immunohistochemical study examining just six cell cycle proteins in HNCs confirmed that these changes in p16 and cyclin D1 expression correlate with HPV status and extend to the protein level (42). In HPV$^+$ cancers, p16 up-regulation and cyclin D1 down-regulation are thought to be a consequence of feedback loops from E7 inhibition of Rb activity (43). For many HPV$^-$ cancers, including HPV$^-$ HNCs (44), reduced p16 expression correlates with p16 promoter hypermethylation, whereas cyclin D1 overexpression is linked to gene amplification (45). p16 repression and cyclin D1 overexpression each predispose mice to multiple cancers, which for cyclin D1 include oral cancers (46).

The distinct expression profile of cell cycle regulatory genes in HPV$^+$ cancers correlated with a higher frequency of PCNA-positive cells (Fig. 4), indicating that HPV$^+$ cancers are more proficient in inducing DNA replication/cell proliferation. Such a virus-induced, highly proliferative state may be responsible for the greater responsiveness of HPV$^+$ HNCs to radiation therapy (15). Overall, these results enhance the potential for E7 inhibition or radiation and anti-DNA replication chemotherapy as treatments for HPV$^+$ cancers.

A subgroup of HPV$^+$ cancers, including HPV$^+$ HNCs and cervical cancers, was distinguished by altered expression of many genes including some associated with B

[10]Strati and Lambert, personal communication.

lymphocytes/lymphomas or endothelial cells (Supplementary Fig. S4C; Supplementary Tables S7). Absence of multiple circulating B-cell markers, including CD19, CD20, and immunoglobulins (28), indicated that this signature was not due to infiltrating lymphocytes. Overexpression of cell migration regulator synaptopodin (29) and some other factors suggested that this class might be associated with increased invasiveness. However, because this subgroup α has more non–laser capture microdissection samples (3 of 6) than subgroup β (2 of 10), we cannot exclude the possibility that microdissection contributes to these subgroup-specific gene expression patterns.

Up-regulation of testis-specific genes in HPV$^+$ HNC and cervical cancer

More than 40 testis antigens normally expressed only in germ line cells have been found in tumors, and many have been linked to cancer-related functions in gene expression, apoptosis, cell differentiation, etc. (47). We found that HPV$^+$ cancers overexpress novel testis antigens *SYCP2*, *STAG3*, and *TCAM1* (Fig. 2A, set III;Table 3). *STAG3* and *SYCP2*, an *SYCP1* homologue, are components of the meiotic synaptonemal complex that promotes recombination (48,49), and *SYCP1* expression induces formation of a synaptonemal complex-like structure (50). Aberrant expression of these meiosis-specific proteins in HPV$^+$ cancers may contribute to the genomic instability induced by high-risk HPVs (51) and to further genetic changes during HPV-associated cancer development. The reduced expression of *SYCP2* in cervical cancer–derived cell line CaSki, relative to early passage HPV16-positive NIKS cells, may reflect some selective disadvantage to long-term, high-level expression of this meiosis-specific gene, perhaps due to recognition as a tumor-specific antigen or interference with normal cell proliferation.

SYCP2 and *TCAM1* were induced by HPV16 in human foreskin keratinocytes and cervical keratinocytes within a few cell passages, and this induction was dependent on E6 and E7 (Fig. 5A and C). *TCAM1* (52), in particular, could be a useful biomarker and therapeutic target as it is expressed on the cell surface and thus is directly accessible.

Supplementary Material

Refer to Web version on PubMed Central for supplementary material.

Acknowledgments

Grant support: NIH grants CA22443 (P. Ahlquist and P.F. Lambert), CA97944 (P. Ahlquist), DE017315 (P.F. Lambert), CA64364 (M.A. Newton), DE15944 (E.M. Smith), CA078609 (K.T. Kelsey), CA100679 (K.T. Kelsey), and CA101873 (C.D. Woodworth).

We thank Bill Sugden and Allan Hildesheim for critical comments, Henry Pitot and Andreas Friedl for pathology assistance, Adam Steinberg and Leanne Olds for illustration support, Aloysius Klingelhutz (Department of Microbiology, University of Iowa, Iowa City, IA) for providing us HPV-transfected cervical epithelial cells, and the National Disease Research Interchange and Gynecologic Oncology Group for providing some tissue samples as indicated.

References

1. Burd EM. Human papillomavirus and cervical cancer. Clin Microbiol Rev 2003;16:1–17. [PubMed: 12525422]
2. Gillison ML, Lowy DR. A causal role for human papillomavirus in head and neck cancer. Lancet 2004;363:1488–9. [PubMed: 15135592]
3. Smith EM, Ritchie JM, Summersgill KF, et al. Human papillomavirus in oral exfoliated cells and risk of head and neck cancer. J Natl Cancer Inst 2004;96:449–55. [PubMed: 15026470]
4. Hunter KD, Parkinson EK, Harrison PR. Profiling early head and neck cancer. Nat Rev Cancer 2005;5:127–35. [PubMed: 15685196]

5. Chung CH, Parker JS, Karaca G, et al. Molecular classification of head and neck squamous cell carcinomas using patterns of gene expression. Cancer Cell 2004;5:489–500. [PubMed: 15144956]
6. Cromer A, Carles A, Millon R, et al. Identification of genes associated with tumorigenesis and metastatic potential of hypopharyngeal cancer by microarray analysis. Oncogene 2004;23:2484–98. [PubMed: 14676830]
7. Ginos MA, Page GP, Michalowicz BS, et al. Identification of a gene expression signature associated with recurrent disease in squamous cell carcinoma of the head and neck. Cancer Res 2004;64:55–63. [PubMed: 14729608]
8. Slebos RJ, Yi Y, Ely K, et al. Gene expression differences associated with human papillomavirus status in head and neck squamous cell carcinoma. Clin Cancer Res 2006;12:701–9. [PubMed: 16467079]
9. Hebner CM, Laimins LA. Human papillomaviruses: basic mechanisms of pathogenesis and oncogenicity. Rev Med Virol 2006;16:83–97. [PubMed: 16287204]
10. Geng Y, Eaton EN, Picon M, et al. Regulation of cyclin E transcription by E2Fs and retinoblastoma protein. Oncogene 1996;12:1173–80. [PubMed: 8649818]
11. Ohtani K, Iwanaga R, Nakamura M, et al. Cell growth-regulated expression of mammalian MCM5 and MCM6 genes mediated by the transcription factor E2F. Oncogene 1999;18:2299–309. [PubMed: 10327050]
12. Thomas, M.; Pim, D.; Banks, L. The role of the HPV E6 oncoprotein in malignant progression. In: Campo, MS., editor. Papillomavirus research. Norfolk (England): Caister Academic Press; 2006. p. 115-31.
13. McCance, DJ. The biology of the E7 protein of HPV-16. In: Campo, MS., editor. Papillomavirus research. Norfolk (England): CaisterAcademic Press; 2006. p. 133-44.
14. Riley RR, Duensing S, Brake T, Munger K, Lambert PF, Arbeit JM. Dissection of human papillomavirus E6 and E7 function in transgenic mouse models of cervical carcinogenesis. Cancer Res 2003;63:4862–71. [PubMed: 12941807]
15. Hoffmann M, Gorogh T, Gottschlich S, et al. Human papillomaviruses in head and neck cancer: 8 year-survival-analysis of 73 patients. Cancer Lett 2005;218:199–206. [PubMed: 15670897]
16. Nielsen HB, Wernersson R, Knudsen S. Design of oligonucleotides for microarrays and perspectives for design of multi-transcriptome arrays. Nucleic Acids Res 2003;31:3491–6. [PubMed: 12824351]
17. Ihaka R, Gentleman R. R: A language for data analysis and graphics. J Comput Graph Stat 1996;5:299–314.
18. Gentleman RC, Carey VJ, Bates DM, et al. Bioconductor: open software development for computational biology and bioinformatics. Genome Biol 2004;5:R80. [PubMed: 15461798]
19. Irizarry RA, Hobbs B, Collin F, et al. Exploration, normalization, and summaries of high density oligonucleotide array probe level data. Biostatistics 2003;4:249–64. [PubMed: 12925520]
20. Efron, B.; Tibshirani, R. An introduction to the bootstrap. New York: Chapman & Hall; 1993.
21. Storey JD, Tibshirani R. Statistical significance for genomewide studies. Proc Natl Acad Sci U S A 2003;100:9440–5. [PubMed: 12883005]
22. Sengupta S, den Boon JA, Chen IH, et al. Genome-wide expression profiling reveals EBV-associated inhibition of MHC class I expression in nasopharyngeal carcinoma. Cancer Res 2006;66:7999–8006. [PubMed: 16912175]
23. Newton MA, Quintana FA, den Boon JA, Sengupta S, Ahlquist P. Random-set methods identify distinct aspects of the enrichment signal in gene-set analysis. Ann Appl Stat. 2007 In press.
24. Ledoit O, Wolf M. A well-conditioned estimator for large-dimensional covariance matrices. J Multivariate Anal 2004;88:365–411.
25. Nelson JH, Hawkins GA, Edlund K, et al. A novel and rapid PCR-based method for genotyping human papillomaviruses in clinical samples. J Clin Microbiol 2000;38:688–95. [PubMed: 10655368]
26. Walboomers JM, Meijer CJ. Do HPV-negative cervical carcinomas exist? J Pathol 1997;181:253–4. [PubMed: 9155707]

27. Khan J, Simon R, Bittner M, et al. Gene expression profiling of alveolar rhabdomyosarcoma with cDNA microarrays. Cancer Res 1998;58:5009–13. [PubMed: 9823299]
28. Clark EA, Lane PJ. Regulation of human B-cell activation and adhesion. Annu Rev Immunol 1991;9:97–127. [PubMed: 1910693]
29. Asanuma K, Yanagida-Asanuma E, Faul C, Tomino Y, Kim K, Mundel P. Synaptopodin orchestrates actin organization and cell motility via regulation of RhoA signalling. Nat Cell Biol 2006;8:485–91. [PubMed: 16622418]
30. Tinker AV, Boussioutas A, Bowtell DD. The challenges of gene expression microarrays for the study of human cancer. Cancer Cell 2006;9:333–9. [PubMed: 16697954]
31. Chung CH, Parker JS, Ely K, et al. Gene expression profiles identify epithelial-to-mesenchymal transition and activation of nuclear factor-{κ}B signaling as characteristics of a high-risk head and neck squamous cell carcinoma. Cancer Res 2006;66:8210–8. [PubMed: 16912200]
32. Brake T, Connor JP, Petereit DG, Lambert PF. Comparative analysis of cervical cancer in women and in a human papillomavirus-transgenic mouse model: identification of minichromosome maintenance protein 7 as an informative biomarker for human cervical cancer. Cancer Res 2003;63:8173–80. [PubMed: 14678972]
33. Longworth MS, Wilson R, Laimins LA. HPV31 E7 facilitates replication by activating E2F2 transcription through its interaction with HDACs. EMBO J 2005;24:1821–30. [PubMed: 15861133]
34. Arroyo M, Bagchi S, Raychaudhuri P. Association of the human papillomavirus type 16 E7 protein with the S-phase-specific E2F-cyclin A complex. Mol Cell Biol 1993;13:6537–46. [PubMed: 8413252]
35. Flores ER, Allen-Hoffmann BL, Lee D, Lambert PF. The human papillomavirus type 16 E7 oncogene is required for the productive stage of the viral life cycle. J Virol 2000;74:6622–31. [PubMed: 10864676]
36. Asano M, Wharton RP. E2F mediates developmental and cell cycle regulation of ORC1 in *Drosophila*. EMBO J 1999;18:2435–48. [PubMed: 10228158]
37. Yamada M, Sato N, Taniyama C, Ohtani K, Arai K, Masai H. A 63-base pair DNA segment containing an Sp1 site but not a canonical E2F site can confer growth-dependent and E2F-mediated transcriptional stimulation of the human ASK gene encoding the regulatory subunit for human Cdc7-related kinase. J Biol Chem 2002;277:27668–81. [PubMed: 12015319]
38. Thacker SA, Bonnette PC, Duronio RJ. The contribution of E2F-regulated transcription to Drosophila PCNA gene function. Curr Biol 2003;13:53–8. [PubMed: 12526745]
39. Furukawa Y, Terui Y, Sakoe K, Ohta M, Saito M. The role of cellular transcription factor E2F in the regulation of cdc2 mRNA expression and cell cycle control of human hematopoietic cells. J Biol Chem 1994;269:26249–58. [PubMed: 7929342]
40. Skoczylas C, Henglein B, Rundell K. PP2A-dependent transactivation of the cyclin A promoter by SV40 ST is mediated by a cell cycle-regulated E2F site. Virology 2005;332:596–601. [PubMed: 15680424]
41. Strati K, Pitot HC, Lambert PF. Identification of biomarkers that distinguish HPV-positive versus HPV-negative head and neck cancers in a mouse model. Proc Natl Acad Sci U S A 2006;103:14152–7. [PubMed: 16959885]
42. Li W, Thompson CH, Cossart YE, et al. The expression of key cell cycle markers and presence of human papillomavirus in squamous cell carcinoma of the tonsil. Head Neck 2004;26:1–9. [PubMed: 14724900]
43. Khleif SN, DeGregori J, Yee CL, et al. Inhibition of cyclin D-CDK4/CDK6 activity is associated with an E2F-mediated induction of cyclin kinase inhibitor activity. Proc Natl Acad Sci U S A 1996;93:4350–4. [PubMed: 8633069]
44. Kraunz KS, Hsiung D, McClean MD, et al. Dietary folate is associated with p16(INK4A) methylation in head and neck squamous cell carcinoma. Int J Cancer 2006;119:1553–7. [PubMed: 16646054]
45. Bartkova J, Lukas J, Muller H, Strauss M, Gusterson B, Bartek J. Abnormal patterns of D-type cyclin expression and G1 regulation in human head and neck cancer. Cancer Res 1995;55:949–56. [PubMed: 7850812]

46. Opitz OG, Harada H, Suliman Y, et al. A mouse model of human oral-esophageal cancer. J Clin Invest 2002;110:761–9. [PubMed: 12235107]
47. Simpson AJ, Caballero OL, Jungbluth A, Chen YT, Old LJ. Cancer/testis antigens, gametogenesis and cancer. Nat Rev Cancer 2005;5:615–25. [PubMed: 16034368]
48. Offenberg HH, Schalk JA, Meuwissen RL, et al. SCP2: a major protein component of the axial elements of synaptonemal complexes of the rat. Nucleic Acids Res 1998;26:2572–9. [PubMed: 9592139]
49. Prieto I, Suja JA, Pezzi N, et al. Mammalian STAG3 is a cohesin specific to sister chromatid arms in meiosis I. Nat Cell Biol 2001;3:761–6. [PubMed: 11483963]
50. Ollinger R, Alsheimer M, Benavente R. Mammalian protein SCP1 forms synaptonemal complex-like structures in the absence of meiotic chromosomes. Mol Biol Cell 2005;16:212–7. [PubMed: 15496453]
51. Duensing S, Munger K. Mechanisms of genomic instability in human cancer: insights from studies with human papillomavirus oncoproteins. Int J Cancer 2004;109:157–62. [PubMed: 14750163]
52. Ono M, Nomoto K, Nakazato S. Gene structure of rat testicular cell adhesion molecule 1 (TCAM-1), and its physical linkage to genes coding for the growth hormone and BAF60b, a component of SWI/SNF complexes. Gene 1999;226:95–102. [PubMed: 9889334]
53. Zhang D, Pier T, McNeel DG, Wilding G, Friedl A. Effects of a monoclonal anti-$\alpha_v\beta_3$ integrin antibody on blood vessels—a pharmacodynamic study. Invest New Drugs 2007;25:49–55. [PubMed: 17001523]

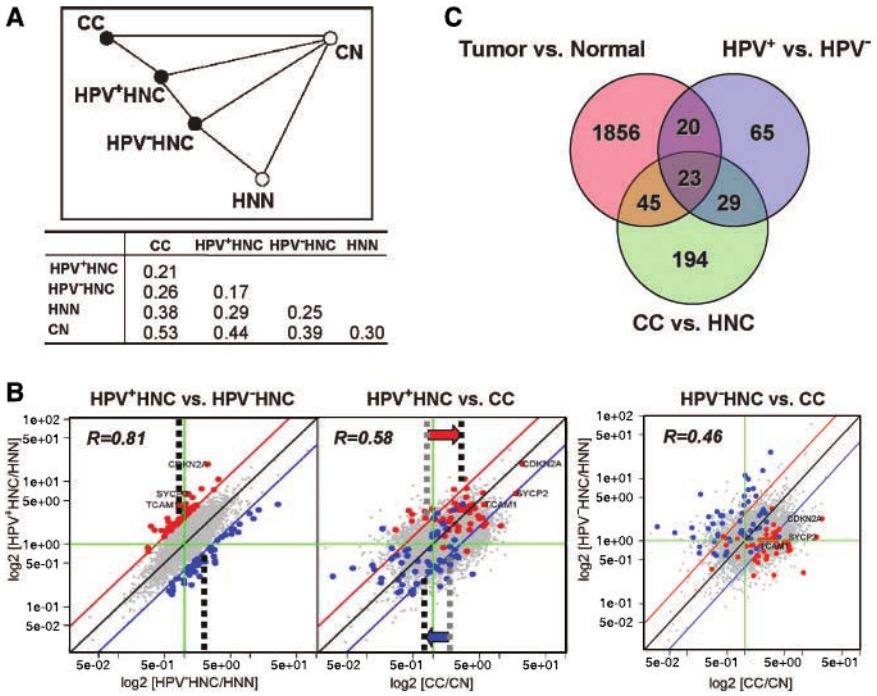

	CC	HPV+HNC	HPV-HNC	HNN
HPV+HNC	0.21			
HPV-HNC	0.26	0.17		
HNN	0.38	0.29	0.25	
CN	0.53	0.44	0.39	0.30

Figure 1.

Global gene expression analysis shows similarities and differences among HPV$^+$ HNC, HPV$^-$ HNC, and cervical cancer. *A*, multidimensional scaling measurements between all indicated pairs of tumor and normal classes of the distances between class-averaged log 2 expression levels over all 54,675 Affymetrix probe sets. The relative distances between each class are approximated in the two-dimensional projection (*top*) and were tabulated *(bottom)*. *CC*, cervical cancer; *CN*, cervical normal. *B*, pairwise comparisons of expression alterations from normal for three cancers are shown as scatter plots of average log 2 fold change from normal. Pearson correlations *(R)* measure global concordance in expression alterations between cancer pairs. Genes that show differential expression between HPV$^+$ HNC and HPV$^-$ HNC are highlighted; tracking into the HPV$^+$ HNC versus HPV$^+$ cervical cancer comparison, these genes are predominantly equivalently expressed between these HPV$^+$ cancers. *Dotted lines*, median expression changes of red and blue genes; *red and blue arrows*, median shifted from HPV$^+$ HNC/HPV$^-$ HNC compared with HPV$^+$ HNC/cervical cancer comparison. *C*, differential expression analysis reveals lists of genes significantly altered between the respective tissue classes. The results of three pairwise comparisons are summarized in the Venn diagram and tabulated fully in Table 3 (HPV$^+$ versus HPV$^-$), Supplementary Table S5 (tumor versus normal), and Supplementary Table S6 (HNC versus cervical cancer).

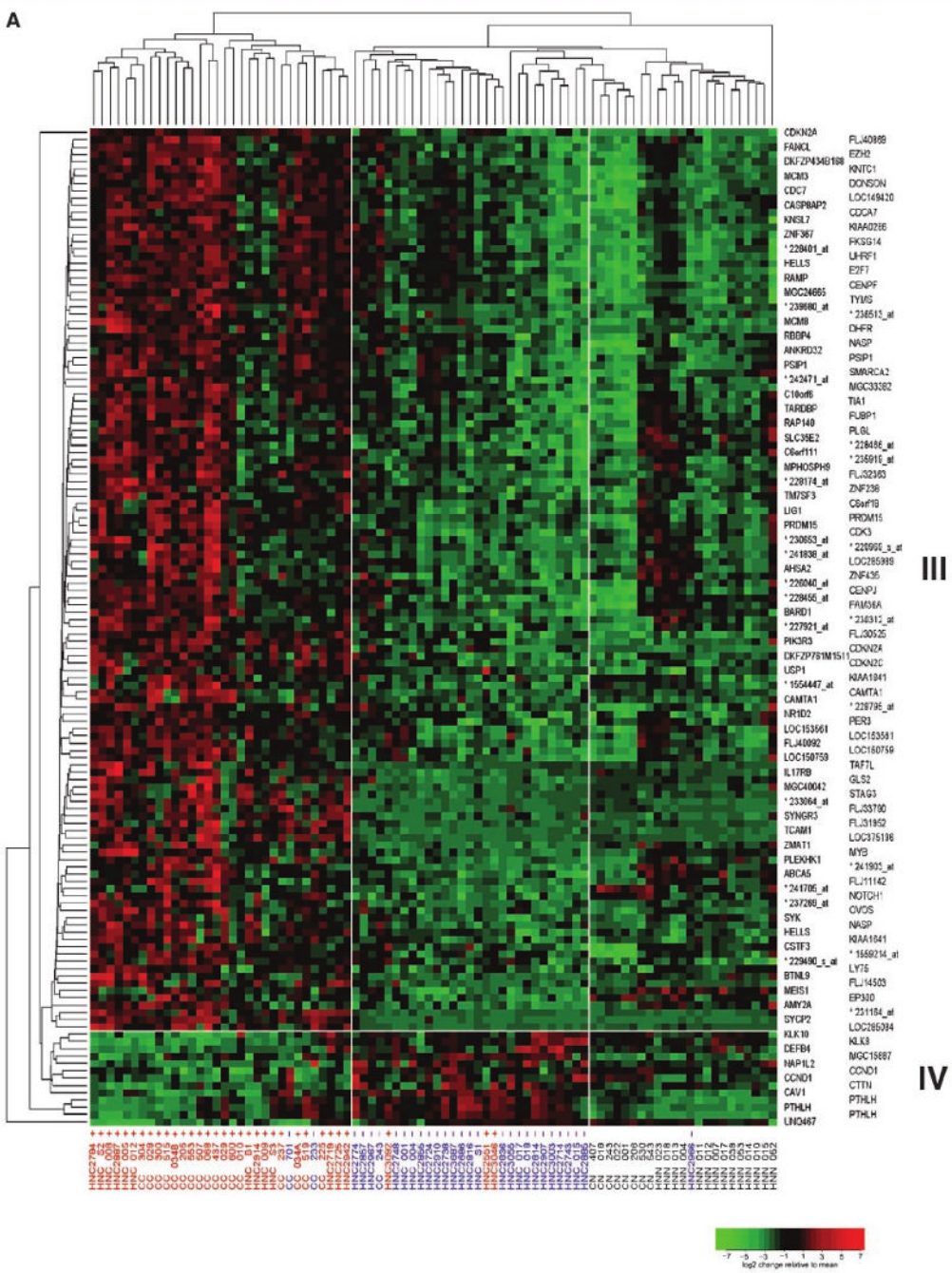

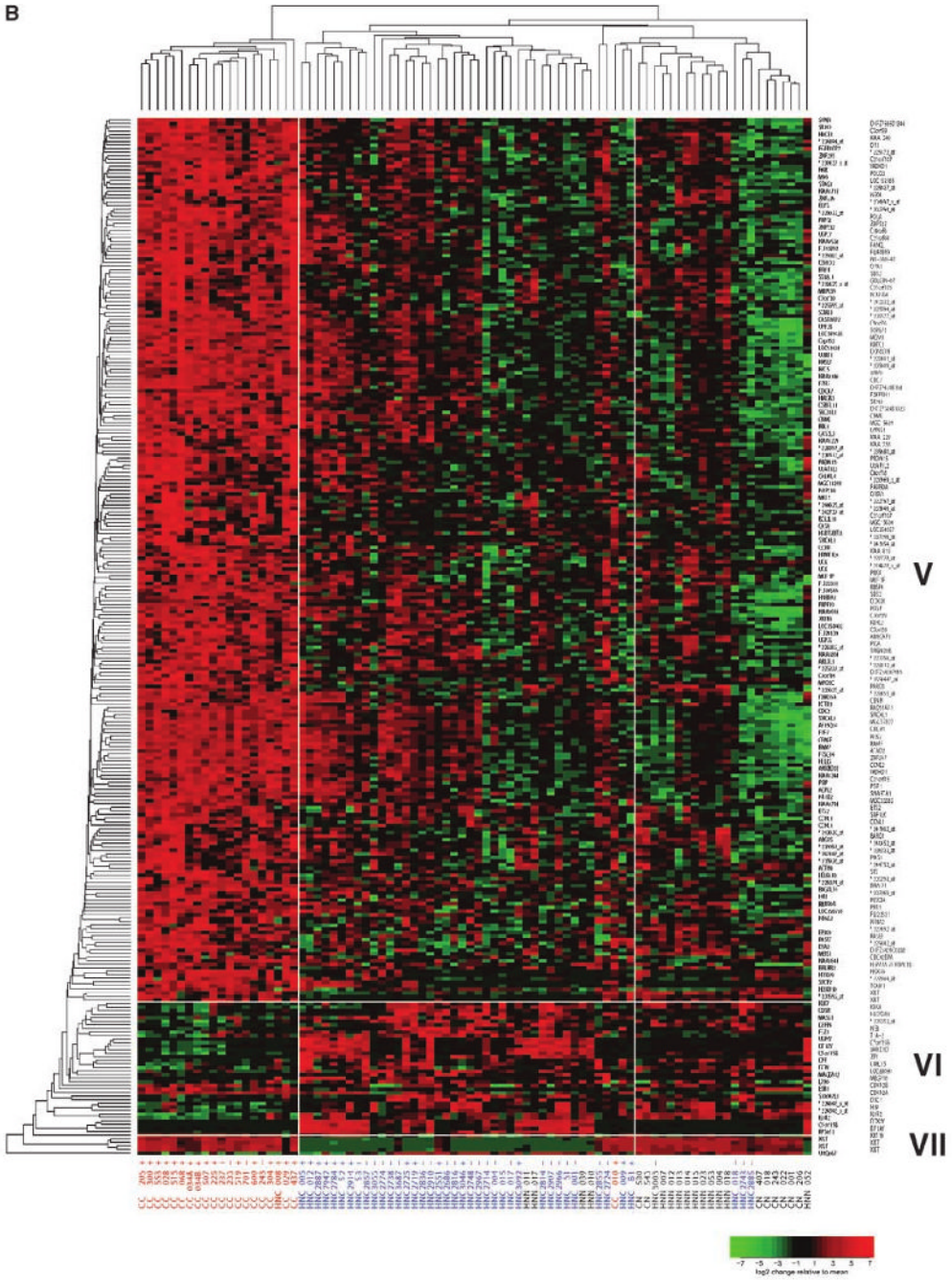

Figure 2.

Gene expression signatures for HPV$^+$ versus HPV$^-$ cancers and HNC versus cervical cancer cancers. *A*, normalized expression values for all 84 samples and 137 probe sets that are significantly differentially expressed between the HPV$^+$ cancers and the HPV$^-$ cancers. *Bottom right key*, high (*red*) and low (*green*) expression, corresponding to a +7.5 to −8.2 log 2 scale of fold change relative to the average of each gene across all 84 microarrays. These genes were ordered by hierarchical clustering based on similarities in their expression changes across the samples (see *dendogram, left*). Gene sets III and IV show significantly up- or down-regulated probe sets, respectively. HPV$^+$ cancer samples (*red text*) and HPV$^-$ cancer samples (*blue text*) are shown at the bottom of the heat map.

B, like *(A)*, but using 291 probe sets that are significantly differentially expressed between cervical cancer and HNC. Gene sets V and VII show significantly up-regulated probe sets in cervical cancer versus HNC, whereas gene set VI shows significantly down-regulated probe sets. Cervical cancer samples *(red text)* and HNC samples *(blue text)* are shown at the bottom of the heat map. *, probe set ID that does not have annotated gene name. HPV status is shown as + and − on each sample ID.

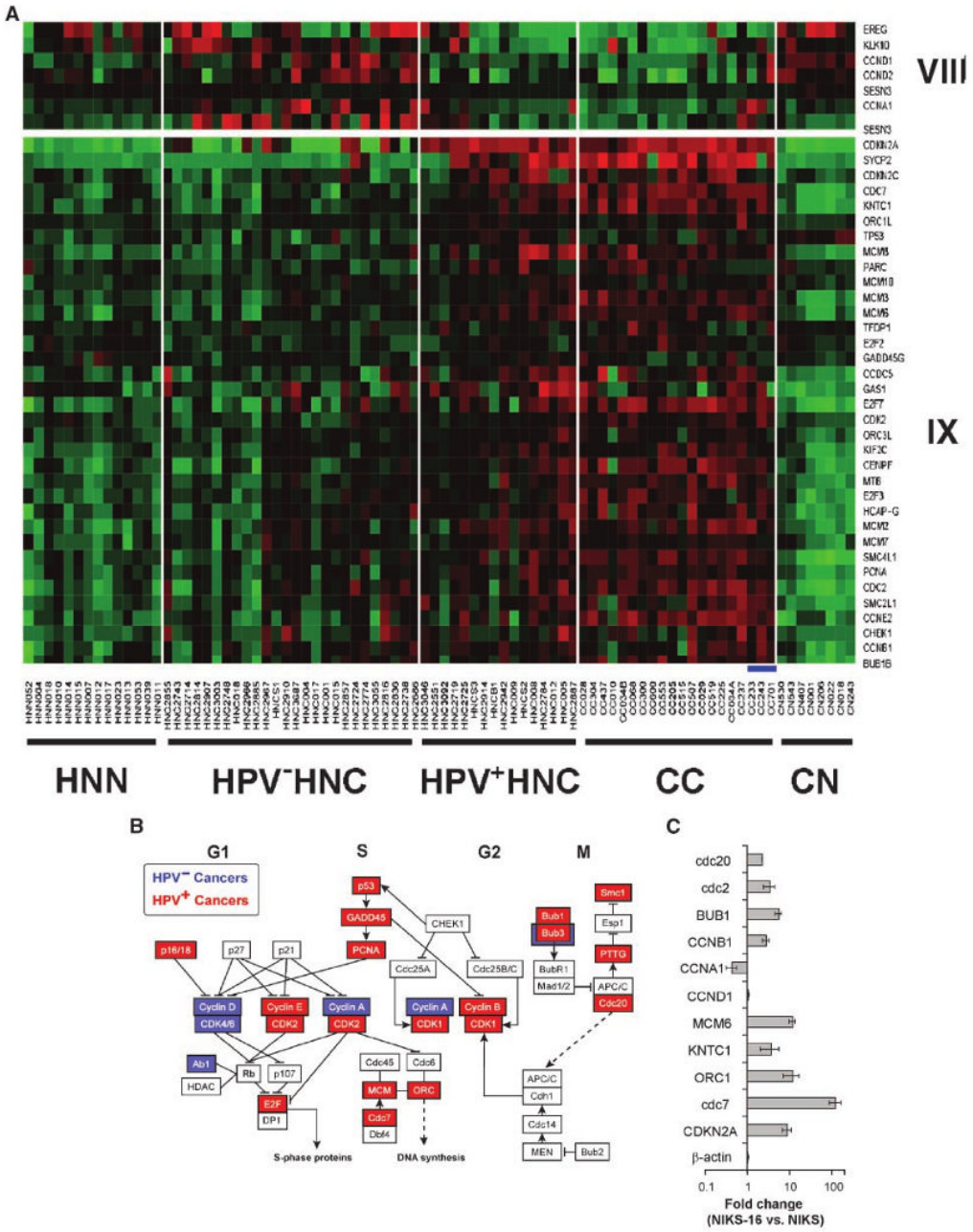

Figure 3.

Cell cycle–related genes are up-regulated in HPV$^+$ cancers. *A*, highly up-regulated genes in HPV$^+$ cancers were analyzed by GO grouping. Cell cycle–related genes were selected and plotted on the heat map. *Blue bars*, HPV$^-$ cervical cancers. *B*, up- and down-regulated genes indicated in the cell cycle pathway provided by the KEGG database. *Red and blue boxes*, up-regulated genes in HPV$^+$ and HPV$^-$ cancers compared with corresponding normal tissue, respectively. *C*, a part of the cell cycle–related genes was analyzed using qRT-PCR. Fold changes of the gene expression in NIKS-16 relative to gene expression in NIKS. *Columns*, mean; *bars*, SD.

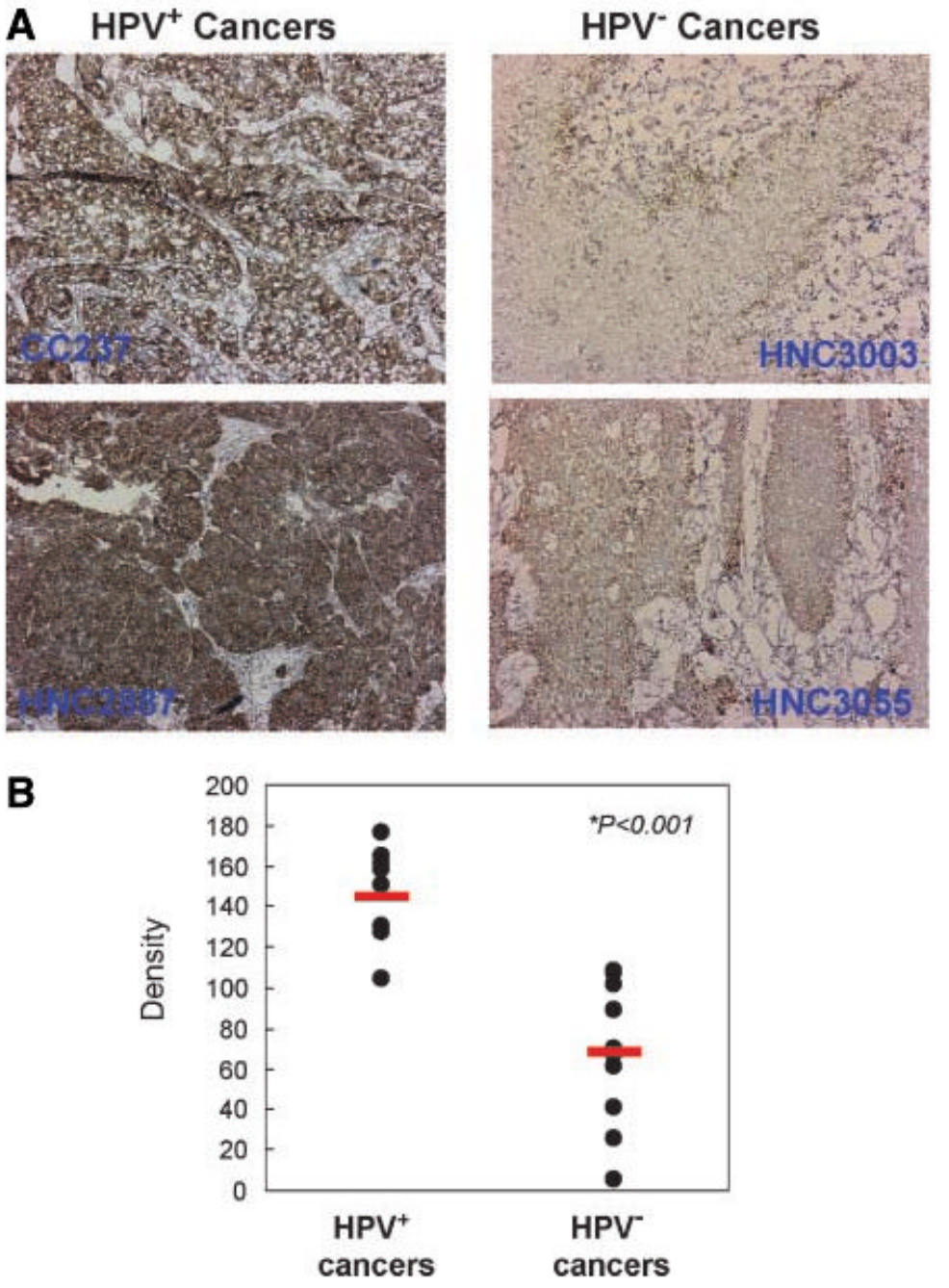

Figure 4.

PCNA protein expression is up-regulated in HPV^+ cancers. Using anti-human PCNA antibody, immunohistochemistry was done with sections of 11 HPV^+ and 10 HPV^- cancers. Immunohistochemical images were analyzed and quantified as described previously (ref. 53; see Supplementary Methods). Representative immunohistochemical images (*A*) and calculated density of all samples (*B*). *Red bars*, mean values of each class. The tissue was also briefly counterstained with hematoxylin.

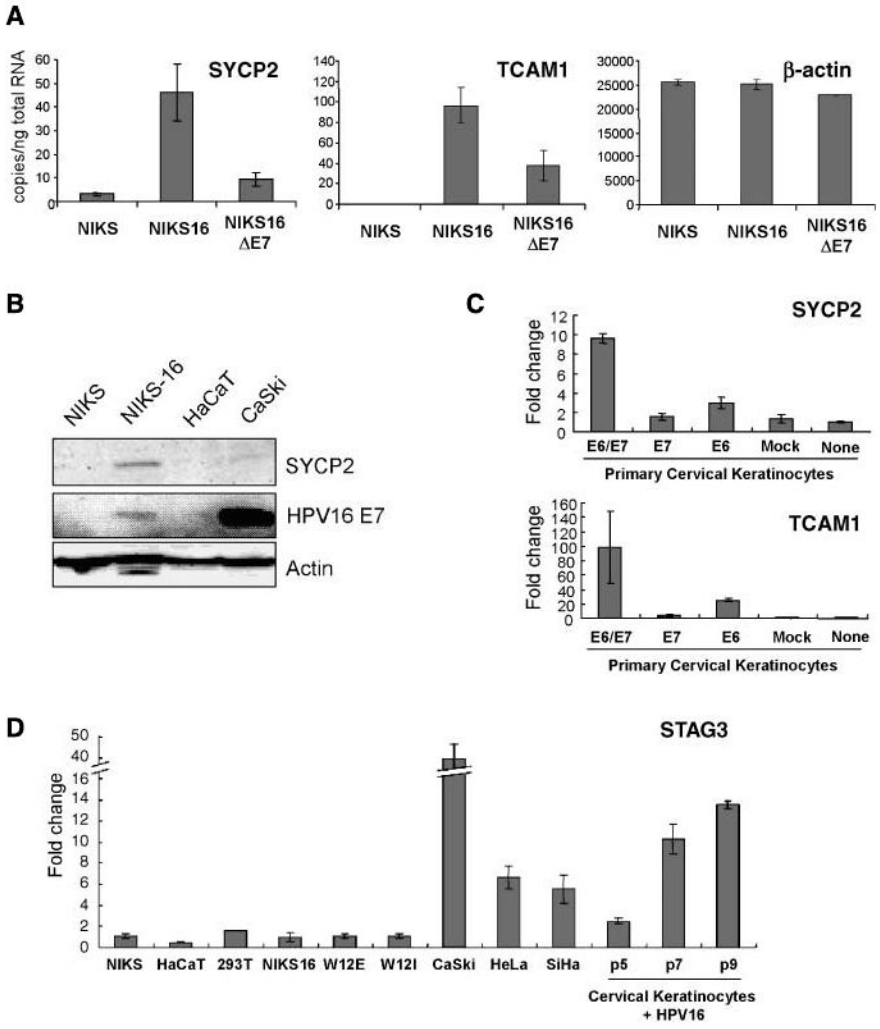

Figure 5.

Testis-specific genes *SYCP2* and *TCAM1* are induced by HPV16. *A*, real-time qRT-PCR was done with total RNA extracted from NIKS cells with and without HPV16. Also, total RNA from NIKS-16 cells without HPV16 E7 protein expression was used to show that testis-specific gene induction by E7 protein was partial. *B*, SYCP2 induction in HPV^{+} cell lines were confirmed with Western blotting using anti-human SYCP2 antibody. Real-time qRT-PCR was done with total RNA extracted from primary cervical keratinocytes with either, or both, HPV16 E6 and E7 delivered by recombinant retrovirus. *C*, retrovirus without *HPV16* gene was used as mock control. *D*, *STAG3* mRNA expression in various cell lines was quantified using qRT-PCR and relative fold change to NIKS cells are plotted. *Columns*, mean; *bars*, SD.

Table 1

Patient information

HNCs		
Cases and controls	***N* = 54/56***	**%**
Case	40	74.1
Control	14	25.9
Age (mean 59.9 ± 15.2), y		
≤55	19	35.2
>55	35	64.8
Gender		
Female	20	37.0
Male	34	63.0
Tumor site		
Oral cavity	32	59.3
Oropharynx	22	40.7
Normal controls only	*N* = 14	%
Age (mean 58.0, ± 23.6), y		
≤55	6	42.9
>55	8	57.1
Gender		
Female	9	64.3
Male	5	35.7
Tumor site		
Oral cavity	9	64.3
Oropharynx	5	35.7
Cases only	*N* = 40/42*	%
Age (mean 60.0 ± 11.3), y		
≤55	13	32.5
>55	27	67.5
Gender		
Female	11	27.5
Male	29	72.5
Tumor site		
Oral cavity	23	57.5
Oropharynx	17	42.5
Stage		
I/II	6	15.0
III	8	20.0
IV	10	25.0
Unknown	16	40.0

HNCs		
Cases and controls	***N* = 54/56***	**%**
Grade		
Poorly/undifferentiated	12	30.0
Well/moderately differentiated	28	70.0
Cervical cancers		
Cases and controls	*N* = 28	%
Case	20	71.4
Control	8	28.5
Age (mean 43.9 ± 10.4), y		
≤45	18	64.3
>45	10	35.7
Normal controls only	*N* =8	%
Age (mean 58.0 ± 23.6), y		
≤45	3	37.5
>45	5	62.5
Cases only	*N* = 20	%
Age (mean 42.5 ± 10.6), y		
≤45	7	35.0
>45	13	67.0
Stage		
IB	16	80.0
II/III	3	15.0
IV	1	5.0
Grade		
Poorly/undifferentiated	12	60.0
Well/moderately differentiated	8	40.0

* Two patients have missing data.

Table 2

HPV status in tumor samples

Diagnosis	Head and neck		Cervix	
	Cancer	Normal	Cancer	Normal
Total	42	14	20	8
HPV negative	26	14	3	8
HPV positive	16	—	17	—
HPV16	13	—	8	—
HPV18	1	—	3	—
HPV31	—	—	1	—
HPV33	2	—	1	—
HPV35	—	—	2	—
HPV58	—	—	1	—
HPV66	—	—	1	—

Table 3

Differentially expressed genes in HPV^+ cancers versus HPV^- cancers

Probe set ID*	Gene title	Gene symbol	*t* statistic	Overlaps†
207039_at	*Cyclin-dependent kinase inhibitor 2A (melanoma, p16, inhibits CDK4)*	*CDKN2A*	6.73	T/N, CC/HNC
228286_at	*Hypothetical protein FLJ40869*	*FLJ40869*	5.45	CC/HNC
218397_at	*Fanconi anemia, complementation group L*	*FANCL*	5.63	CC/HNC
203358_s_at	*Enhancer of zeste homologue 2 (Drosophila)*	*EZH2*	6.41	CC/HNC
218783_at	*DKFZP434B168 protein*	*DKFZP434B168*	6.00	CC/HNC
206316_s_at	*Kinetochore associated 1*	*KNTC1*	6.26	T/N, CC/HNC
201555_at	*MCM3 minichromosome maintenance deficient 3 (S. cerevisiae)*	*MCM3*	5.88	T/N, CC/HNC
221677_s_at	*Downstream neighbor of SON*	*DONSON*	6.08	T/N, CC/HNC
204510_at	*CDC7 cell division cycle 7 (S. cerevisiae)*	*CDC7*	6.42	T/N, CC/HNC
227255_at	*Casein kinase*	*LOC149420*	5.59	CC/HNC
222201_s_at	*CASP8 associated protein 2*	*CASP8AP2*	5.09	T/N, CC/HNC
224428_s_at	*Cell division cycle associated 7*	*CDCA7*	4.36	CC/HNC
219306_at	*Kinesin-like 7*	*KNSL7*	5.45	CC/HNC
212621_at	*KIAA0286 protein*	*KIAA0286*	4.60	T/N
229551_x_at	*Zinc finger protein 367*	*ZNF367*	6.29	T/N, CC/HNC
222848_at	*Leucine zipper protein FKSG14*	*FKSG14*	4.37	T/N, CC/HNC
228401_at	—	—	4.49	T/N, CC/HNC
225655_at	*Ubiquitin-like, containing PHD and RING finger domains, 1*	*UHRF1*	4.69	T/N, CC/HNC
227350_at	*Helicase, lymphoid-specific*	*HELLS*	5.13	T/N, CC/HNC
228033_at	*E2F transcription factor 7*	*E2F7*	4.36	T/N, CC/HNC
218585_s_at	*RA-regulated nuclear matrix-associated protein*	*RAMP*	4.99	T/N, CC/HNC
209172_s_at	*Centromere protein F, 350/400ka (mitosin)*	*CENPF*	4.51	T/N, CC/HNC
226456_at	*Hypothetical protein MGC24665*	*MGC24665*	6.23	T/N
202589_at	*Thymidylate synthetase*	*TYMS*	5.51	T/N
239680_at	—	—	5.19	CC/HNC
236513_at	—	—	4.85	CC/HNC
224320_s_at	*MCM8 minichromosome maintenance deficient 8*	*MCM8*	5.73	T/N
202532_s_at	*Dihydrofolate reductase*	*DHFR*	5.24	None
210371_s_at	*Retinoblastoma binding protein 4*	*RBBP4*	4.73	T/N, CC/HNC
201970_s_at	*Nuclear autoantigenic sperm protein (histone-binding)*	*NASP*	6.42	T/N, CC/HNC
223542_at	*Ankyrin repeat domain 32*	*ANKRD32*	4.40	T/N, CC/HNC
209337_at	*PC4 and SFRS1 interacting protein 1*	*PSIP1*	6.01	CC/HNC
205961_s_at	*PC4 and SFRS1 interacting protein 1*	*PSIP1*	5.59	CC/HNC
206542_s_at	*SWI/SNF related, matrix associated, actin-dep chromatin regulator*	*SMARCA2*	4.88	None
242471_at	—	—	4.97	None
229442_at	*Hypothetical protein MGC33382*	*MGC33382*	4.45	T/N, CC/HNC
203482_at	*Chromosome 10 open reading frame 6*	*C10orf6*	6.24	CC/HNC
201448_at	*TIA1 cytotoxic granule-associated RNA binding protein*	*TIA1*	5.60	None
221264_s_at	*TAR DNA binding protein*	*TARDBP*	5.57	None

Probe set ID*	Gene title	Gene symbol	*t* statistic	Overlaps†
214093_s_at	*Far upstream element (FUSE) binding protein 1*	*FUBP1*	4.78	None
209285_s_at	*Retinoblastoma-associated protein 140*	*RAP140*	5.56	None
230120_s_at	*Plasminogen-like*	*PLGL*	5.39	None
217122_s_at	*Solute carrier family 35, member E2*	*SLC35E2*	7.47	None
228466_at	*Clone IMAGE:111714 mRNA sequence*	—	5.59	None
212179_at	*Chromosome 6 open reading frame 111*	*C6orf111*	5.31	None
235919_at	—	—	5.10	None
215731_s_at	*M-phase phosphoprotein 9*	*MPHOSPH9*	4.64	None
229886_at	*FLJ32363 protein*	*FLJ32363*	5.87	None
228174_at	—	—	6.44	None
212774_at	*Zinc finger protein 238*	*ZNF238*	4.65	None
226478_at	*Transmembrane 7 superfamily member 3*	*TM7SF3*	4.64	None
42361_g_at	*Chromosome 6 open reading frame 18*	*C6orf18*	5.76	CC/HNC
202726_at	*Ligase I, DNA, ATP-dependent*	*LIG1*	6.26	None
231931_at	*PR domain containing 15*	*PRDM15*	7.15	CC/HNC
230777_s_at	*PR domain containing 15*	*PRDM15*	6.54	CC/HNC
229468_at	*Cyclin-dependent kinase 3*	*CDK3*	5.45	None
230653_at	—	—	5.15	None
220969_s_at	—	—	4.93	CC/HNC
241838_at	—	—	4.90	None
235231_at	*Hypothetical protein LOC285989*	*LOC285989*	4.47	None
212980_at	*AHA1, activator of heat shock 90 kDa protein ATPase homologue 2*	*AHSA2*	4.47	None
219676_at	*Zinc finger protein 435*	*ZNF435*	5.16	None
226040_at	*Hypothetical protein LOC283585*	—	4.43	None
223513_at	*Centromere protein J*	*CENPJ*	5.41	T/N, CC/HNC
228455_at	*CDNA FLJ43677 fis, clone SYNOV4009295*	—	5.28	CC/HNC
225786_at	*Family with sequence similarity 36, member A*	*FAM36A*	4.56	CC/HNC
205345_at	*BRCA1-associated RING domain 1*	*BARD1*	5.04	CC/HNC
227921_at	—	—	4.97	None
230312_at	—	—	4.35	None
225841_at	*Hypothetical protein FLJ30525*	*FLJ30525*	6.64	T/N
202743_at	*Phosphoinositide-3–kinase, regulatory subunit 3 (p55, γ)*	*PIK3R3*	5.96	None
209644_x_at	*Cyclin-dependent kinase inhibitor 2A (melanoma, p16, inhibits CDK4)*	*CDKN2A*	6.39	T/N
225355_at	*Hypothetical protein DKFZP761M1511*	*DKFZP761M1511*	5.05	None
204159_at	*Cyclin-dependent kinase inhibitor 2C (p18, inhibits CDK4)*	*CDKN2C*	5.83	None
202412_s_at	*Ubiquitin specific protease 1*	*USP1*	5.55	T/N
243539_at	*KIAA1841 protein*	*KIAA1841*	4.86	None
1554447_at	*CDNA clone MGC:32876 IMAGE:4734912, complete cds*	—	4.53	CC/HNC
213268_at	*Calmodulin-binding transcription activator 1*	*CAMTA1*	5.53	None
1555370_a_at	*Calmodulin-binding transcription activator 1*	*CAMTA1*	4.80	None
229795_at	—	—	4.27	T/N
225768_at	*Nuclear receptor subfamily 1, group D, member 2*	*NR1D2*	4.51	CC/HNC

Probe set ID*	Gene title	Gene symbol	*t* statistic	Overlaps†
221045_s_at	*Period homologue 3 (Drosophila)*	*PER3*	6.43	CC/HNC
232889_at	*Hypothetical protein LOC153561*	*LOC153561*	4.97	None
213089_at	*Hypothetical protein LOC153561*	*LOC153561*	4.58	None
213605_s_at	*FLJ40092 protein*	*FLJ40092*	5.95	None
221973_at	*Hypothetical protein LOC150759*	*LOC150759*	5.14	T/N, CC/HNC
213703_at	*Hypothetical protein LOC150759*	*LOC150759*	5.46	None
220325_at	*TAF7-like RNA polymerase II, TATA box binding protein-associated factor*	*TAF7L*	5.11	None
219255_x_at	*Interleukin 17 receptor B*	*IL17RB*	5.67	None
205531_s_at	*Glutaminase 2 (liver, mitochondrial)*	*GLS2*	4.44	None
230011_at	*Similar to mouse meiosis defective 1 gene*	*MGC40042*	5.34	None
219753_at	*Stromal antigen 3*	*STAG3*	6.09	None
233064_at	*Hypothetical gene supported by AL365406; BC034005*	—	7.85	None
1553611_s_at	*Hypothetical protein FLJ33790*	*FLJ33790*	5.15	None
205691_at	*Synaptogyrin 3*	*SYNGR3*	4.84	T/N
1558217_at	*Hypothetical protein FLJ31952*	*FLJ31952*	4.64	None
233320_at	*Testicular cell adhesion molecule 1*	*TCAM1*	7.07	T/N, CC/HNC
1556244_s_at	*Hypothetical protein LOC375196*	*LOC375196*	7.56	None
226344_at	*Zinc finger, matrin type 1*	*ZMAT1*	5.47	None
204798_at	*v-myb myeloblastosis viral oncogene homologue (avian)*	*MYB*	5.12	None
230469_at	*Pleckstrin homology domain containing, family K member 1*	*PLEKHK1*	6.22	None
241903_at	—	—	5.20	CC/HNC
213353_at	*ATP-binding cassette, subfamily A (ABC1), member 5*	*ABCA5*	4.35	CC/HNC
221103_s_at	*Hypothetical protein FLJ11142*	*FLJ11142*	5.67	None
241705_at	—	—	4.63	None
218902_at	*Notch homologue 1, translocation-associated (Drosophila)*	*NOTCH1*	5.57	None
237269_at	—	—	4.92	CC/HNC
228245_s_at	*Ovostatin*	*OVOS*	4.30	T/N
244023_at	*Spleen tyrosine kinase*	*SYK*	4.98	None
242918_at	*Nuclear autoantigenic sperm protein (histone-binding)*	*NASP*	4.60	None
242890_at	*Helicase, lymphoid-specific*	*HELLS*	4.45	T/N
220940_at	*KIAA1641*	*KIAA1641*	4.22	None
229666_s_at	*Cleavage stimulation factor, 3′ pre-RNA, subunit 3, 77kDa*	*CSTF3*	4.44	None
1559214_at	—	—	4.52	T/N
229490_s_at	—	—	4.32	T/N
205668_at	*Lymphocyte antigen 75*	*LY75*	4.26	None
228434_at	*Butyrophilin-like 9*	*BTNL9*	4.87	None
228262_at	*Hypothetical protein FLJ14503*	*FLJ14503*	5.40	None
204069_at	*Meis1, myeloid ecotropic viral integration site 1 homologue (mouse)*	*MEIS1*	4.97	T/N, CC/HNC
1562921_at	*E1A binding protein p300*	*EP300*	4.28	CC/HNC
208498_s_at	*Amylase, α 2A; pancreatic*	*AMY2A*	5.32	None
231164_at	*Hypothetical gene supported by AK095200; BC042853*	—	6.91	T/N

Probe set ID*	Gene title	Gene symbol	*t* statistic	Overlaps†
206546_at	*Synaptonemal complex protein 2*	*SYCP2*	7.49	T/N, CC/HNC
1557570_a_at	*Hypothetical protein LOC285084*	*LOC285084*	5.88	T/N
209792_s_at	*Kallikrein 10*	*KLK10*	−4.32	None
206125_s_at	*Kallikrein 8 (neuropsin/ovasin)*	*KLK8*	−5.68	CC/HNC
207356_at	*Defensin, β4*	*DEFB4*	−4.28	CC/HNC
226448_at	*Hypothetical gene supported by BC009447*	*MGC15887*	−4.40	T/N
219368_at	*Nucleosome assembly protein 1-like 2*	*NAP1L2*	−5.63	None
208712_at	*Cyclin D1 (PRAD1: parathyroid adenomatosis 1)*	*CCND1*	−4.50	None
208711_s_at	*Cyclin D1 (PRAD1: parathyroid adenomatosis 1)*	*CCND1*	−5.27	None
214073_at	*Cortactin*	*CTTN*	−5.10	None
203065_s_at	*Caveolin 1, caveolae protein, 22 kDa*	*CAV1*	−4.58	T/N
210355_at	*Parathyroid hormone-like hormone*	*PTHLH*	−4.45	T/N
1556773_at	*Parathyroid hormone-like hormone*	*PTHLH*	−4.43	T/N
211756_at	*Parathyroid hormone-like hormone*	*PTHLH*	−4.46	T/N
230835_at	*KIPV467*	*UNQ467*	−4.37	CC/HNC

Abbreviations: T, tumor; N, normal; CC, cervical cancer.

*In order as shown in Fig. 2A.

†Probe sets differentially expressed in other comparisons are indicated as tumor versus normal and cervical cancer versus HNC. Please see Fig. 1C.

Table 4

Cell cycle genes up- or down-regulated in HPV^+ cancers versus HPV^- cancers

Probe set ID*	Gene title	Gene symbol	*t* statistic
205767_at	*Epiregulin*	*EREG*	−3.47
209792_s_at	*Kallikrein 10*	*KLK10*	−4.25
208711_s_at	*Cyclin D1*	*CCND1*	−5.43
208712_at	*Cyclin D2*	*CCND2*	−4.48
1553869_at	*Sestrin 3*	*SESN3*	−3.39
205899_at	*Cyclin A1*	*CCNA1*	−4.06
235683_at	*Sestrin 3*	*SESN3*	−4.05
207039_at	*Cyclin-dependent kinase inhibitor 2A (melanoma, p16, inhibits CDK4)*	*CDKN2A*	7.09
206546_at	*Synaptonemal complex protein 2*	*SYCP2*	7.36
204159_at	*Cyclin-dependent kinase inhibitor 2C (p18, inhibits CDK4)*	*CDKN2C*	5.73
204510_at	*CDC7 cell division cycle 7*	*CDC7*	6.51
206316_s_at	*Kinetochore associated 1*	*KNTC1*	6.28
205085_at	*Origin recognition complex, subunit 1-like*	*ORC1L*	4.96
201746_at	*Tumor protein p53*	*TP53*	3.57
224320_s_at	*MCM8 minichromosome maintenance deficient 8*	*MCM8*	5.61
213204_at	*p53-associated parkin-like cytoplasmic protein*	*PARC*	5.90
222962_s_at	*MCM10 minichromosome maintenance deficient 10*	*MCM10*	2.74
201555_at	*MCM3 minichromosome maintenance deficient 3*	*MCM3*	5.95
201930_at	*MCM6 minichromosome maintenance deficient 6*	*MCM6*	5.56
244550_at	*Transcription factor Dp-1*	*TFDP1*	3.00
228361_at	*E2F transcription factor 2*	*E2F2*	4.94
204121_at	*Growth arrest and DNA-damage-inducible, γ*	*GADD45G*	2.16
225297_at	*Coiled-coil domain containing 5 (spindle associated)*	*CCDC5*	3.42
204457_s_at	*Growth arrest-specific 1*	*GAS1*	2.17
228033_at	*E2F transcription factor 7*	*E2F7*	4.39
204252_at	*Cyclin-dependent kinase 2*	*CDK2*	3.77
210028_s_at	*Origin recognition complex, subunit 3-like (yeast)*	*ORC3L*	4.12
209408_at	*Kinesin family member 2C*	*KIF2C*	5.52
209172_s_at	*Centromere protein F, 350/400ka (mitosin)*	*CENPF*	4.55
219588_s_at	*Leucine zipper protein 5*	*LUZP5*	4.86
203693_s_at	*E2F transcription factor 3*	*E2F3*	4.05
218663_at	*Chromosome condensation protein G*	*HCAP-G*	3.55
202107_s_at	*MCM2 minichromosome maintenance deficient 2, mitotin*	*MCM2*	4.37
208795_s_at	*MCM7 minichromosome maintenance deficient 7*	*MCM7*	4.06
201664_at	*SMC4 structural maintenance of chromosomes 4-like 1*	*SMC4L1*	4.44
201202_at	*Proliferating cell nuclear antigen*	*PCNA*	5.12
203213_at	*Cell division cycle 2, G1 to S and G_2 to M*	*CDC2*	3.27
204240_s_at	*SMC2 structural maintenance of chromosomes 2-like 1*	*SMC2L1*	1.73
205034_at	*Cyclin E2*	*CCNE2*	3.59

Probe set ID*	Gene title	Gene symbol	*t* statistic
205393_s_at	*CHK1 checkpoint homologue*	*CHEK1*	1.05
214710_s_at	*Cyclin B1*	*CCNB1*	1.20
203755_at	*BUB1 budding uninhibited by benzimidazoles 1 homologue β*	*BUB1B*	2.77

* In order as shown in Fig. 3A.